♦ Optimization of Unicast Services Transmission for Broadcast Channels in Practical Situations

Zeina Mheich, Marie-Line Alberi Morel, and Pierre Duhamel

The problem of constellation shaping for broadcast transmission in degraded channels remains a challenge. This is especially so when a single source communicates simultaneously with two receivers using a finite dimension constellation. This paper focuses on a practical situation where unicast service to each user is transmitted over broadcast channels. We investigate the optimization of an achievable rate closure region by using non-uniform constellations issued from superimposition of high-rate information on low-rate information and by using a nonequiprobable distribution of the transmitted symbols. The achievable rate region is derived for a two-user additive white Gaussian noise (AWGN) broadcast channel and for finite input pulse amplitude modulation (PAM) constellations. A noticeable shaping gain up to 3.5 dB maximum was shown on signal-to-noise ratio (SNR), compared with the equiprobable distribution of transmitted symbols obtained for a 4-PAM constellation when achievable rates are maximized over the probability distribution of channel input signals and the constellation shape.

Introduction

Mobile access networks (e.g., Long Term Evolution (LTE)/Third Generation (3G)) have enabled the emergence of multiple video-oriented mobile services including non-linear services such as video on demand (VoD) and catch-up television (TV), as well as linear or near-live services such as live or Internet TV. In addition, the proliferation of highly "smart" mobile phones and portable devices has led to a significant increase in the demand for data services [5]. Consequently, users have to stream or to download video-oriented services through shared networks which need to fully exploit their already restricted spectrum resources. Optimal radio resource sharing techniques are highly desirable for mobile operators in order to enable all these devices to be connected over wireless networks, with a pre-defined guaranteed quality of service.

In the 1970s, Cover [6] demonstrated that in the case of an additive white Gaussian noise (AWGN) broadcast channel, the simultaneous transmission of superimposed information from one source to multiple users achieves better spectrum efficiency compared with time-sharing or other orthogonal division schemes for allocating channel resources among users.

Bell Labs Technical Journal 17(1), 5–24 (2012) © 2012 Alcatel-Lucent. Published by Wiley Periodicals, Inc.
Published online in Wiley Online Library (wileyonlinelibrary.com) • DOI: 10.1002/bltj.21521

Panel 1. Abbreviations, Acronyms, and Terms

3D—Three dimensional
3G—Third Generation
AWGN—Additive white Gaussian noise
BC—Broadcast channel
BS—Base station
CSI—Channel state information
DVB—Digital Video Broadcasting
DVB-H—DVB to handhelds
DVB-SH—DVB satellite services to handhelds
DVB-T—DVB terrestrial
HM—Hierarchical modulation
IFFT—Inverse fast Fourier transform
ITU—International Telecommunication Union
ITU-T—ITU Telecommunication Standardization Sector
LSB—Least significant bit
LTE—Long Term Evolution
MS—Modulation superposition
MSB—Most significant bit
MSEQ—Modulation superposition with equiprobable symbols
OFDMA—Orthogonal Frequency Division Multiple Access
PAM—Pulse amplitude modulation
QAM—Quadrature amplitude modulation
SC—Superposition coding
SCOP—SC optimized
SIC—Successive interference cancelation
SINR—Signal-to-interference-plus-noise ratio
SNR—Signal-to-noise ratio
TV—Television
VoD—Video on demand

Bergmans and Cover demonstrated further that superposition coding reaches the theoretical capacity limit for a two-user additive white Gaussian noise channel using an infinite Gaussian input alphabet [2].

Motivated by these remarkable results, practical implementation of superposition coding known as hierarchical modulation (HM) or layered modulation has been included in various standards including Digital Video Broadcast for terrestrial television (DVB-T) [7], DVB to handhelds (DVB-H), and DVB satellite services to handhelds (DVB-H/SH) for mobile digital TV transmission [8] of broadcast scalable digital media [17]. Hierarchical modulation enables the transmission of two independent broadcast service streams on a single frequency radio channel, with different transmission qualities (signal-to-noise ratio (SNR) scalability) over non-uniform 16-quadrature amplitude modulation (QAM) constellations. Various resource sharing strategies exploiting the broadcast nature of the wireless channel have been investigated and found to be useful for enhancing the cell downlink spectral efficiency for wireless networks that use orthogonal transmission schemes (either in time and/or frequency) and for addressing multiple receivers. Systems relying on superposition coding for time-frequency multiple access are investigated for Orthogonal Frequency Division Multiple Access (OFDMA) schemes in [1, 14, and 15]. Results on superposition coding for a downlink broadcast channel are covered in [13] and [21]. The authors explain how an advantage in diversity of radio conditions over a cell is transformed into an improvement in SNR.

However, real transmission systems impose the use of finite input alphabets which, are usually fed with equiprobable symbols. As a consequence, previous results which deal mainly with theoretical information limits, do not apply straightforwardly in practical situations. Indeed, these restrictions contribute to introduce a gap between the capacity region achieved with infinite Gaussian inputs for the AWGN channel and the throughputs obtained in practical situations. This gap can be reduced by using constellation shaping, which was developed on the premise that signals with a large norm are used less frequently than signals with a small norm [9]. One approach to obtain a shaping gain in the AWGN channel is to arrange the constellation points in such a way that the channel input distribution is closer to a Gaussian shape, i.e., with more points at the lower power levels and fewer at higher power levels. Another approach is to transmit finite-size uniformly-spaced symbols with low energy more frequently (near the origin) than the ones with high energy (far from the origin). Using non-uniform signals reduces the entropy of the transmitter output, and hence, the achievable rate. However, the expectation is to compensate the loss in achievable rate with bit error savings for better protection against channel noise symbols with low energy, which are selected more frequently than symbols with large energy.

In fact, for constellations with finite dimensions, most results available dealing with optimal constellation shape or with optimal probability distribution of symbols consider only unicast transmission, where one transmitter communicates with one receiver. For example, [16] and [23] investigate the design of an optimal non-uniform constellation using signals with equal probability but unequal spacing. [22] shows that using non-uniform signal sets in high order modulation schemes could result in gains of about 1 dB over an AWGN channel. In [3] and [18] the authors obtain a shaping gain by arranging points in such a way that the emitted signal is closer to a Gaussian distribution. Constellation shaping known as *shell mapping* is specified in International Telecommunication Union Telecommunication Standardization Sector (ITU-T) recommendation V.34 [12], and was initially applied in the V.34 data modem. In [20], the authors describe a shaping gain between 0.8 dB to 1.0 dB on average transmitted power that can be obtained within constellations divided into a set of several rings by selecting a sequence of rings whose points reduce the constellation expansion ratio, or the peak average power ratio. In [19], the authors investigate the effects of the nonequiprobable distribution of M-ary QAM signal constellation points on the error performance for nonlinear channels. Simulations for binary turbo coded modulation show a 3 dB improvement over equiprobable symbols. In [11], the authors studied the achievable rates in a two-user AWGN broadcast channel when superposition techniques are applied, assuming a uniform probability density function over the finite input set. To our knowledge, no work investigating the maximization of achievable rates for broadcast transmission considering optimization over both the probability density and constellation symbols have been reported. Since this joint optimization was shown to be useful in a unicast transmission situation, our paper intends to evaluate its impact in the context of broadcast transmission. We are specifically interested in the superposition coding technique as a broadcast transmission method. This paper attempts to maximize the achievable rate closure region for a finite-size constellation when superposition coding is applied to transmitted data. This maximization is based on the joint optimization of the constellation shape and of the probability distribution of the transmitted symbols for a two-user AWGN broadcast channel, which is referred to as a degraded channel. We focus on a 4-pulse amplitude modulation (PAM) constellation, which is compliant with the modulation schemes standardized for wireless radio interfaces.

The paper is organized as follows. In the section immediately following, we present a scenario for resource sharing using superposition coding for mobile unicast services in the downlink. We consider a broadcast transmission of two unicast services, referred to as private messages. Next, we derive achievable rates using the mutual information for a two-user AWGN broadcast channel when the transmit signal is modulated with a 4-PAM constellation. The calculations are done in the transmission scheme of modulation superposition using equiprobable symbols, which represents a particular case of superposition coding. Furthermore, a discussion about the labeling schemes and about the joint probability distribution schemes highlights the fact that the well-known hierarchical modulation represents a particular case of modulation superposition. We then optimize the achievable rate closure region by taking into account all possible labeling schemes for a 4-PAM constellation and the general case of superposition coding. For target achievable rates, our numerical results show noticeable shaping gain on SNR up to 3.5 dB at maximum and up to 1.2 dB in mean for a 4-PAM constellation.

Superposition Coding as Method of Resource Sharing for Mobile Unicast Services

Superposition coding as a method of resource sharing for mobile unicast services is illustrated in **Figure 1**. The superposition coding (SC) technique

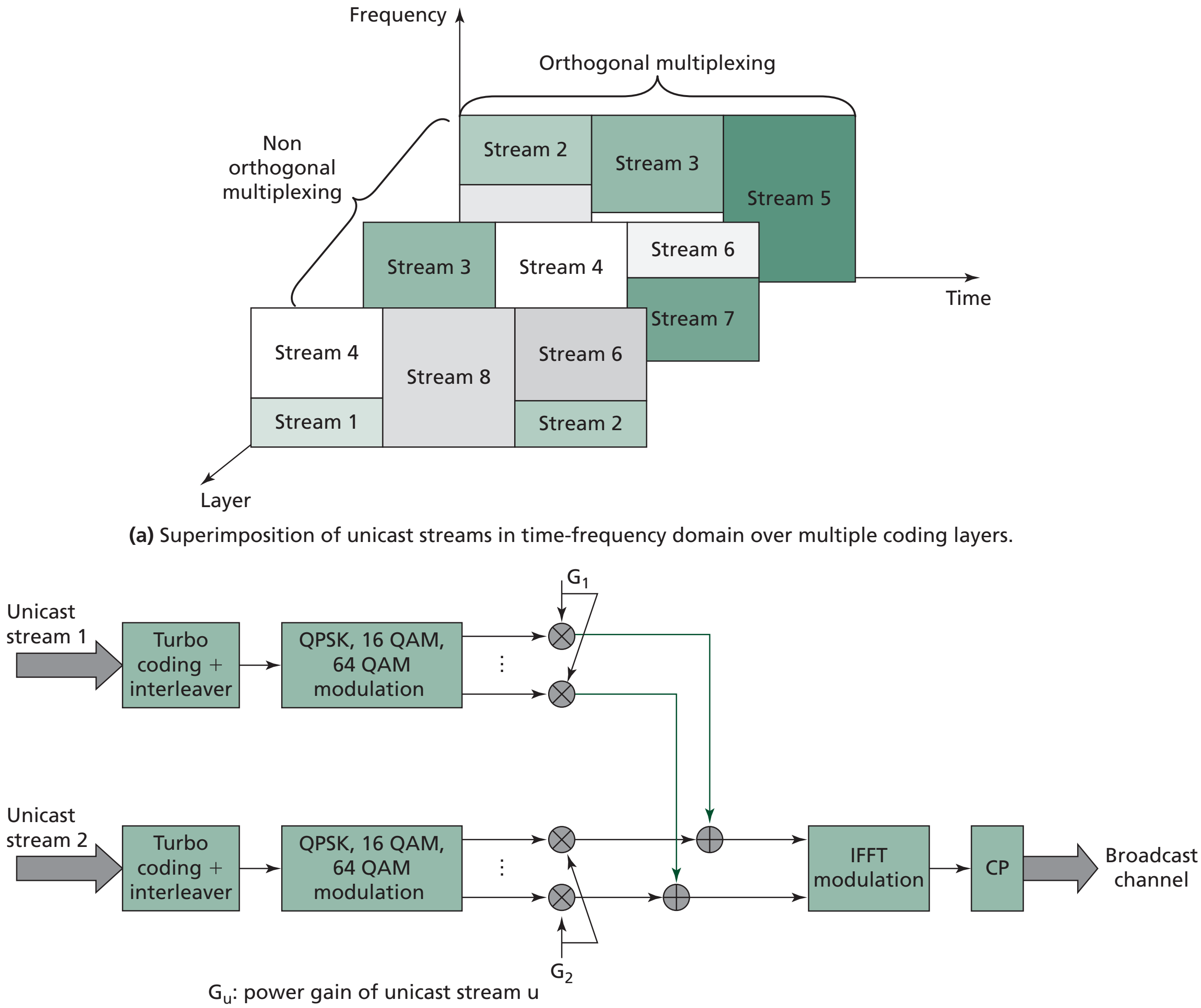

(a) Superimposition of unicast streams in time-frequency domain over multiple coding layers.

(b) Block diagram of two independent unicast stream superimposition in the OFDM transmitter.

CP—Cyclic prefix
IFFT—Inverse fast Fourier transform
OFDM—Orthogonal Frequency Division Multiple Access
QAM—Quadrature amplitude modulation
QPSK—Quadrature phase shift keying

Figure 1.
Superposition coding as a method of resource sharing for mobile unicast services.

consists of superimposing several independent streams intended for different users with the aim of transmitting them simultaneously on the same radio resources in the same time slot (time-frequency resource in a frame) as shown in Figure 1a. This technique enables operators to improve the cell spectral efficiency without the need for additional antennas and with very little feedback and channel information since it depends on long-term channel statistics only. In this way, SC introduces an additional dimension in the resource sharing space. Contrary, however, to time-frequency multiple access schemes, SC lends itself to non-orthogonal sharing since the streams overlap in both the time and frequency domain. The resulting three-dimensional (3D) multiplexing scheme thus relies on adopting an Orthogonal Frequency Division Multiple Access (OFDMA) downlink transmission scheme for the LTE radio interface. The superimposition of the independent streams is achieved in the transmitter in the frequency domain before the inverse fast Fourier transform (IFFT). As an example, Figure 1b provides a possible implementation of the superimposition of two independent streams in an OFDM physical layer. From a practical view point, the number of streams superimposed and transmitted in the same radio broadcast channel is restricted to two in order to limit the complexity of SC implementation in the transmitter and the receiver [10]. Hence, this paper considers the case in which a sender simultaneously transmits two superimposed independent streams destined for two receivers.

Consider the following scenario for *downlink unicast services*. An infrastructure-based network comprises a base station (BS) that wishes to communicate with a plurality of users and thus needs to send different unicast streams in the downlink channel. We suppose that some receivers are much closer to the BS ("good" users) than others ("bad" users), whose receivers are near the cell edge for example. The good users exhibit an SNR higher than the bad users. Instead of transmitting the different unicast streams in different radio resources (time-frequency slots in a frame) with different radio throughputs, the BS partially superimposes the streams for transmission on the same radio resource. Users that have to be served at the cell edge generally exhibit bad channel conditions and tend to waste a significant amount of resources since the BS has to serve them at low transmission rate. The superimposition of high-rate information and low-rate information thus reduces the amount of unused resources in the broadcast channel and consequently improves the cell's spectral efficiency. On the receiver side, a successive interference cancelation (SIC) receiver is required. For "good" users, the mobile devices will decode the unicast stream after cancelling interference from the other streams. In contrast, the mobile devices of "bad" users simply treat the superimposed additional signal as interference.

The achievable rates for both good users and bad users depend on the SNR at the receiver. Superposition coding provides a gain in throughput compared to that of a time-frequency multiplexing scheme when users with larger differences in signal-to-interference-plus-noise ratio (SINR) are paired in the same broadcast channel [15]. The choice of optimal pairs is determined at the transmitter side from the channel state information (CSI) sent by the receivers. The power allocated to each stream is also a determining factor [11]. To allow both signals to be decoded, the power level allocated to two paired users has to be adjusted accordingly. Consequently, the BS scheduler includes the constraint of a large SNR gap and power sharing between the two paired users in order to select optimal couples of users to maximize throughput over the broadcast channel. This is illustrated in **Figure 2**.

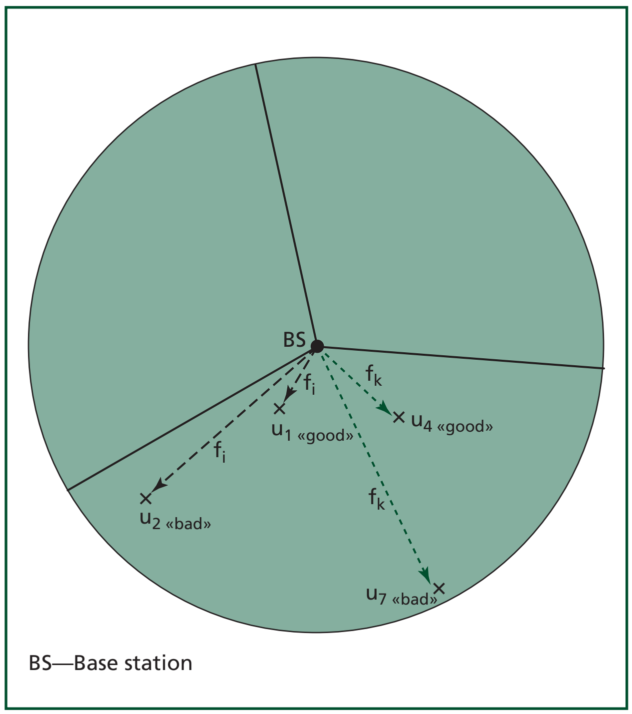

Figure 2.
Pairing example of good and bad users in the same downlink broadcast channel within a cell.

Private Message Achievable Rates for Two-User AWGN Broadcast Channel

The scenario for *downlink unicast services* is represented by "private message" transmission over a broadcast channel in information theory.

In a two-user broadcast channel (BC), the transmitted signal X (drawn from the alphabet $\mathcal{X}$) is sent to user 1 and user 2, which receive, respectively, the signals Y_1 and Y_2 belonging to the alphabets $\mathcal{Y}_1$ and $\mathcal{Y}_2$. A broadcast channel is said to be physically degraded i $X \to Y_1 \to Y_2$ forms a Markov chain, i.e., Y_2 is a "degraded′" version of the signal Y_1. The two-user AWGN broadcast channel (AWGN BC) is described by,

$$Y_1 = X + N_1 \tag{1}$$

$$Y_2 = X + N_2 \tag{2}$$

where N_1 and N_2 are zero-mean Gaussian variables whose respective variances satisfy $\sigma_1^2 < \sigma_2^2$. A physically degraded BC can be constructed equivalently to the AWGN BC by introducing a new independent noise $N_3 \sim \mathcal{N}(0, \sigma_2^2 - \sigma_1^2)$. The transmission of private messages over a two-user AWGN broadcast channel is depicted by the schematic block diagram in **Figure 3**. The transmitted signal X represents the jointly encoded signal of two individual private messages. X depends on the signal X_1 transporting the private message for user 1 and on the signal U carrying the private message for user 2. At the receiver, user 1 and user 2 independently decode their respective private messages from channel outputs Y_1 and Y_2, with no collaboration between them. More precisely, user 1 and user 2 are independent and do not communicate with each other.

R_1 and R_2 respectively define the private message achievable rate for user 1 and user 2. The set of pairs (R_1, R_2) satisfies

$$R_1 \leq (X; Y_1 | U) \tag{3}$$

$$R_2 \leq I(U; Y_2) \tag{4}$$

for any given joint probability distribution $P_{UXY_1Y_2} = P_{UX} \cdot P_{Y_1|X} \cdot P_{Y_2|X}$ on $\{\mathcal{U} \times \mathcal{X} \times \mathcal{Y}_1 \times \mathcal{Y}_2\}$.

- $I(X; Y_1|U)$ represents the mutual information between the transmit signal X and the received signal Y_1 after U is observed.
- $I(U; Y_2)$ denotes the mutual information between the auxiliary random variable U and the received signal Y_2.

P_{UX} is the joint probability distribution of U and X. $P_{Y_1|X}$ and $P_{Y_2|X}$ are the conditional distributions that depend on the nature of the channel.

From the inequality shown in equation 4, $I(U;Y_2)$ is the maximal rate achievable by user 2. Hence the second receiver can only distinguish U, where the

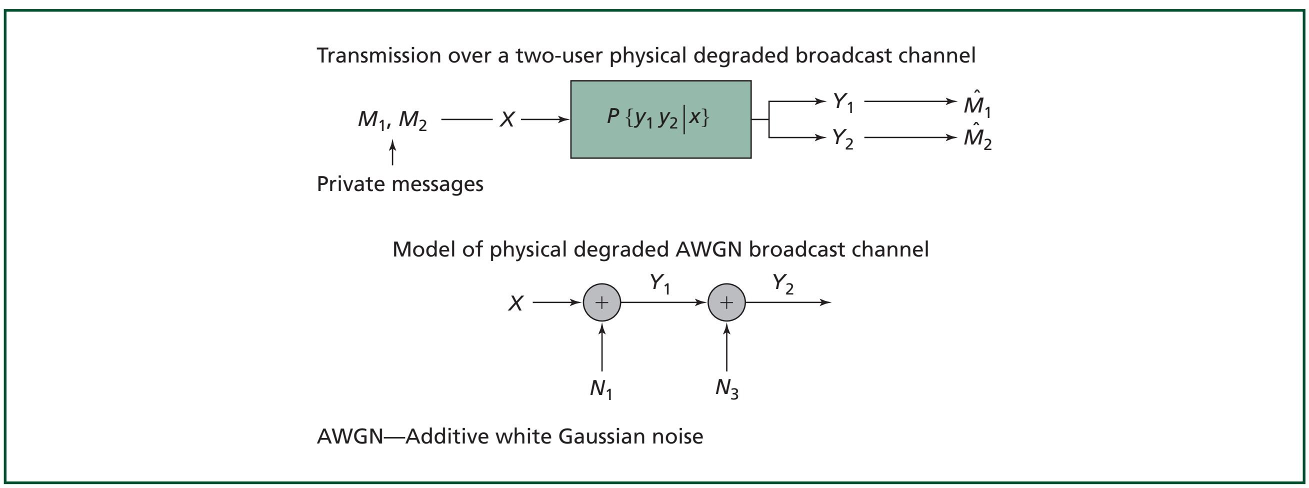

Figure 3.
Scheme for transmission of private messages over a two-user physical degraded broadcast channel.

alphabet U has cardinality bounded by $|\mathcal{U}| \leq \min\{|\mathcal{X}|, |\mathcal{Y}_1|, |\mathcal{Y}_2|\}$.

The message U is always decoded first by both users. In the case of user 1, U is also subtracted from the received signal Y_1, which cancels the interference such that the message X_1 can be then detected.

The mutual information $I(U; Y_2)$ and $I(X; Y_1|U)$ between the input and the output of a transmission corrupted by AWGN is given by the following formulas,

$$I(X; Y_1|U) = \sum_{u,x,y_1} P_{UX}(u,x) P_{Y_1|X}(y_1|x) \cdot \log \frac{\left(\sum_{x'} P_{UX}(u,x')\right) P_{Y_1|X}(y_1|x)}{\sum_{x'} P_{UX}(u,x') P_{Y_1|X}(y_1|x')}$$

$$I(U; Y_2) = \sum_{u,y_2} \left(\sum_{x} P_{UX}(u,x) P_{Y_2|X}(y_2|x) \right) \cdot \log \frac{\sum_{x'} P_{UX}(u,x') P_{Y_2|X}(y_2|x')}{\left(\sum_{x'} P_{UX}(u,x')\right)\left(\sum_{u',x'} P_{UX}(u',x') P_{Y_2|X}(y_2|x')\right)} \quad (5)$$

where the transition probability function $P_{Y_i|X}(y_i|x)$ is expressed in the case of the AWGN channel as,

$$P_{Y_i|X}(y_i|x) = \frac{1}{\sqrt{2 \cdot \pi \cdot \sigma_i^2}} \cdot \exp\left(-\frac{(y_i - x)^2}{2\sigma_i^2}\right) \quad (6)$$

The capacity region for the stochastically degraded Gaussian BC, which is defined as the set of all simultaneously achievable communication rate pairs, is known. The theoretical limit of the capacity region of a two-user Gaussian broadcast channel is achieved when the transmitter uses superposition coding on two Gaussian infinite alphabet signals intended for the two users [2, 6].

In the following section, the private message achievable rates are derived in the case of non-uniform 4-PAM constellation when "private" signals are equiprobable and are added in the modulation space before transmission. This way of superimposing signals is referred to as *modulation superposition* (MS).

Superposition Coding With Finite-Size Constellations by Adding Private Signals: Modulation Superposition

Modulation superposition corresponds to the addition of both signals, X_1 and U, such that $X = X_1 + U$. The signal intended for user 1 and user 2 are binary, and are simply added. We derive the private message achievable rates for user 1 and user 2 in a 4-PAM.

For a 4-PAM transmission, $X \in X = \{x_0, x_1, x_2, x_3\}$. The signals Y_1 and Y_2 received respectively by user 1 and user 2 are continuous in the case of an AWGN channel, and thus $|\mathcal{Y}_1| = |\mathcal{Y}_2| = \infty$. As a consequence, $|\mathcal{U}|$ is bounded by $\min\{|\mathcal{X}|\}$. For transmission with a 4-PAM constellation $|\mathcal{X}| = 4$, thus $|\mathcal{U}| \leq 4$. We consider the case $|\mathcal{U}| = 2$. Thus user 2 can receive at most 1 bit/channel since it can distinguish only U. User 1 also receives two symbols, thus at most 1 bit/channel. This reception mode is also practical because in such a case each user uses the same constellation to modulate their information which will ease the eventual implementation.

The 4-PAM transmission is performed under the following constraints:

- The sum of the joint probabilities p_{ij} should be equal to 1,
- The transmitted signal should have zero mean: $E[x] = 0$,
- The power of the transmitter signal should be limited: $E\lfloor x^2 \rfloor = P$.

The constraints on the values of the symbols in $\mathcal{X}$ and the joint probability distribution $P_{UX}(u, x)$ are given by,

$$\sum_{i,j} p_{ij} = 1, \sum_{i,j} p_{ij} \cdot x_j = 0, \sum_{i,j} p_{ij} \cdot x_j^2 = P. \quad (7)$$

Private Message Achievable Rates in a 4-PAM Constellation for Modulation Superposition Using Equiprobable Symbols

Consider alphabets $\mathcal{X}_1$ and $\mathcal{X}_2$ with average powers P_1 and P_2 corresponding to user 1 and user 2 respectively. The encoded bit stream is modulated using $\mathcal{X}_k$ with $k = \{1, 2\}$ and generates symbols, which is a sequence of 2 signal points $\{x_{kl}\}$ where $x_{kl} \in \mathcal{X}_k$.

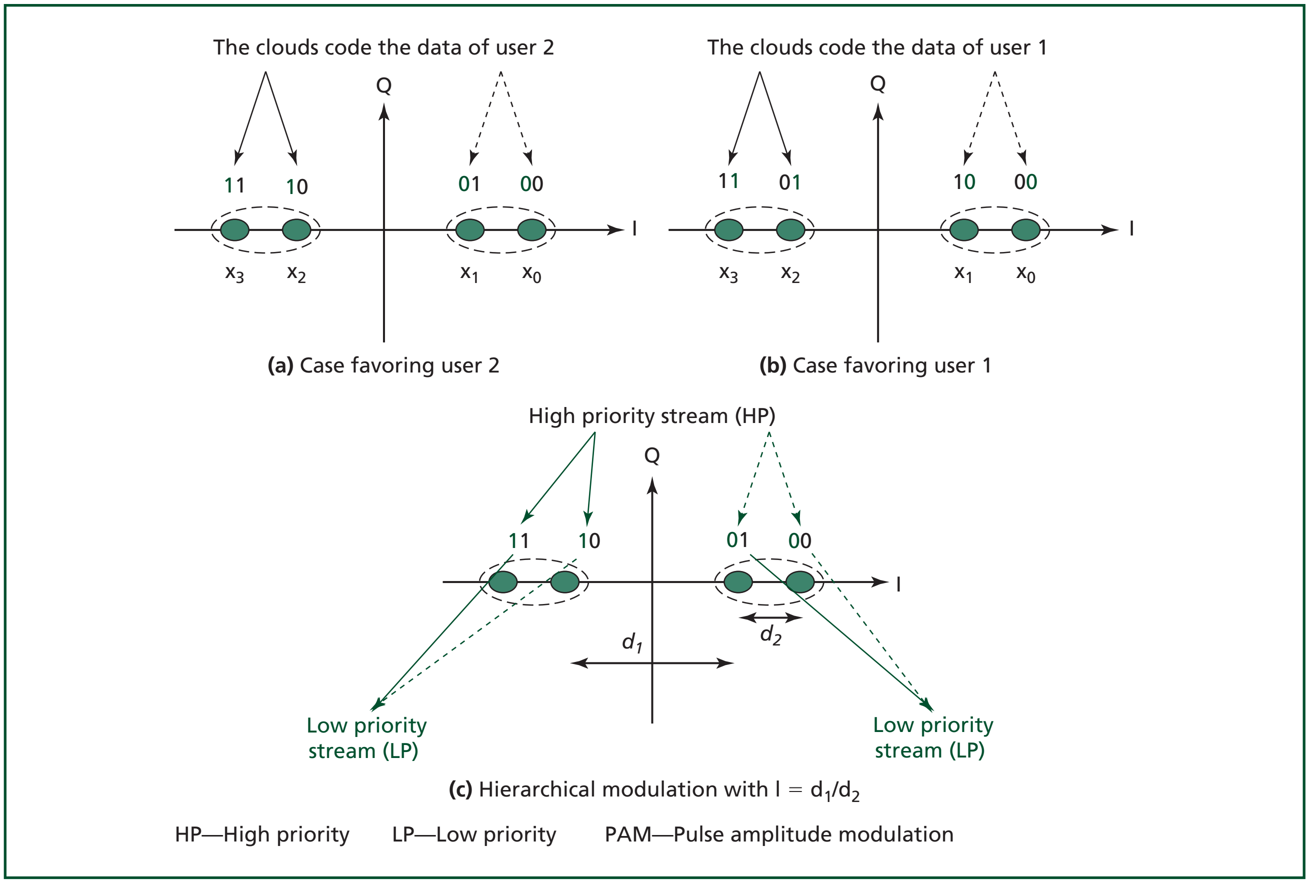

Figure 4.
Labeling schemes for 4-PAM when using modulation superposition.

The messages for both users are encoded separately and added before transmission. The signal on the channel reads $x = x_{1l} + x_{2n} \in \mathcal{X}$, where $l, n \in \{0, 1\}$. Each alphabet is thus composed of two symbols such that $\mathcal{X}_1 = \{x_{10}, x_{11}\}$ and $\mathcal{X}_2 = \{x_{20}, x_{21}\}$, where $x_{k1} = -x_{k0}$. Symbols are taken equiprobably from these two alphabets so their average power is given by $P_1 = x_{10}^2$ and $P_2 = x_{20}^2$. We now add the symbols from these two binary alphabets which results in a 4-PAM constellation whose symbols $\{x_0, x_1, x_2, x_3\}$ are equiprobable and symmetric ($x_0 = -x_3$ and $x_1 = -x_2$) and verify $x_0 = x_{10} + x_{20}$ and $x_3 = x_{11} + x_{21}$ where $x0 \geq x_1 \geq x_2 \geq x_3$. The total transmission power P is split between both users so that a power $P_1 = \alpha \cdot P$, with $\alpha \subset ([0, 1]$ allocated to user 1 and $P_2 = (1 - \alpha) \cdot P$ to user 2. Then, per [21], x_0 is expressed as,

$$x_0 = \sqrt{\alpha \cdot P} + \sqrt{(1 - \alpha) \cdot P} \tag{8}$$

and x_1 is expressed as,

$$\begin{aligned} x_1 &= \sqrt{\alpha \cdot P} - \sqrt{(1 - \alpha) \cdot P} \quad && \text{if } \alpha \geq 0.5 \\ x_1 &= -\sqrt{\alpha \cdot P} + \sqrt{(1 - \alpha) \cdot P} \quad && \text{if } \alpha \leq 0.5 \end{aligned} \tag{9}$$

Adding constellations whose symbols are equiprobable will be denoted by modulation superposition with equiprobable symbols.

Figure 4 shows labeling schemes for a 4-PAM when using modulation superposition. The addition of two binary alphabets results in a 4-PAM constellation with only two possible labeling schemes (depicted in Figure 4a and Figure 4b), which represents the distribution of the 2-bit words over the four constellation symbols. In both labeling schemes, user 2 is always mapped to the most significant bit (MSB) and user 1 is always mapped to the least significant bit (LSB). Both schemes differ in the mapping of the codewords '01' and '10' over the symbols x_1 and x_2. They are swapped in the two configurations. In Figure 4a the codewords {'00', '01'} and {'11', '10'} with the same MSB are mapped over the symbols located in the same half plane. In this configuration, the half plane carries user 2's information while the dots inside the half plane carry the data of user 1. Clearly, the labeling scheme depicted in Figure 4a favors the detection of user 2's information since the symbol clusters are more protected against the channel noise than the dots of the cluster. In Figure 4b the codewords with the same LSB are located in the same region. Therefore, the labeling scheme depicted in this figure favors the detection of user 1's information.

The labeling scheme is imposed by $P_{UX}(u, x)$ which establishes the connections between the elements of U and the elements of X. In the case of an equiprobable distribution, each connection is marked with the uniform probability of 1/4. $P_{UX}(u, x)$ is thus limited to the two following cases, shown in **Figure 5**:

1. $p_{00} = p_{01} = p_{11} = p_{13} = 0.25$ when $\alpha \leq 0.5$ which yields the joint probability distribution scheme shown in Figure 5a (corresponding to the labeling scheme of Figure 4a), or
2. $p_{00} = p_{02} = p_{11} = p_{13} = 0.25$ when $\alpha \geq 0.5$ which yields the joint probability distribution scheme shown in Figure 5b (corresponding to the labeling scheme of Figure 4a).

Figure 4c depicts the labeling scheme used by hierarchical modulation (HM). We observe that this is similar to the scheme shown in Figure 4a. HM represents a particular case of modulation superposition using equiprobable symbols, more precisely when $\alpha \leq 0.5$. The parameter α thus becomes the only parameter which affects the form of the region of the achievable rates. This is indeed the approach adopted in industry standards for DVB since detection is simplified with the scheme shown in Figure 4a. It is easy to see, for example, that when $\alpha < 0.5$, the positive values of the received signal Y_2 may be directly related to $X_2 = x_{20}$, and the negative values to $X_2 = x_{21}$.

According to P_{UX} schemes and the constellation symbol expressions in equation 8 and equation 9, the mutual information $I(X; Y_1|U)$ of user 1 and $I(U; Y_2)$ of user 2 is thus derived from equation 5 as a function of α (see the **Appendix**). As a consequence, the achievable rate closure region is obtained by varying α from 0 to 1.

The achievable rate closure region obtained with finite-size constellations is lower than the capacity closure region. In the next section, we investigate if the achievable rate closure region obtained with a 4-PAM constellation can be enhanced by jointly optimizing the constellation shape and the symbol probability distribution. The maximization procedure

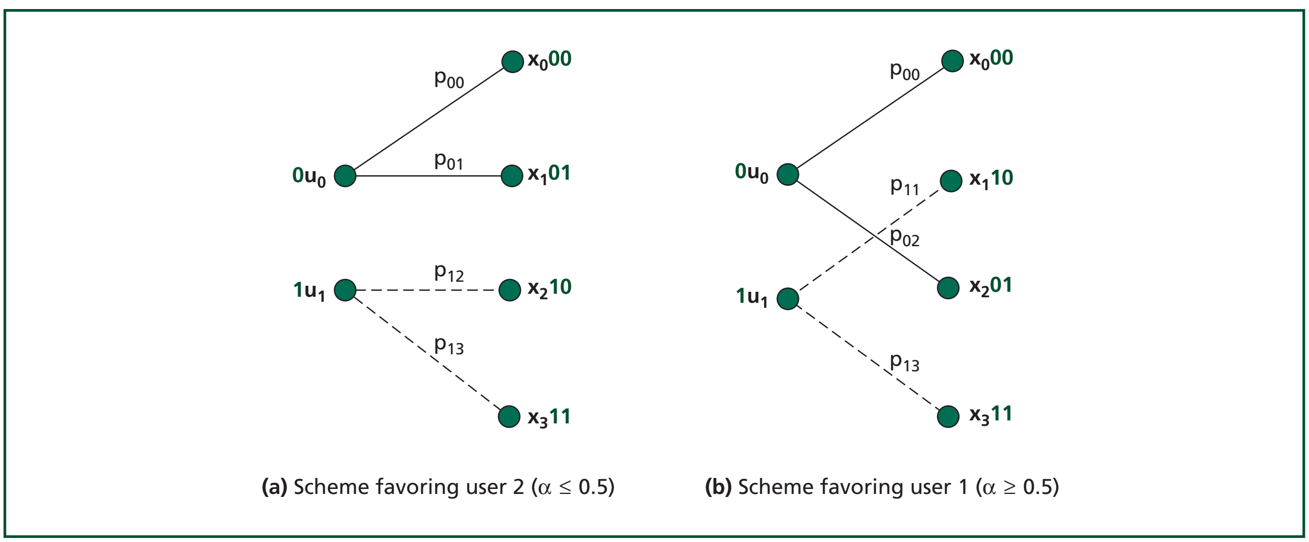

Figure 5.
Joint probability distribution of U and X.

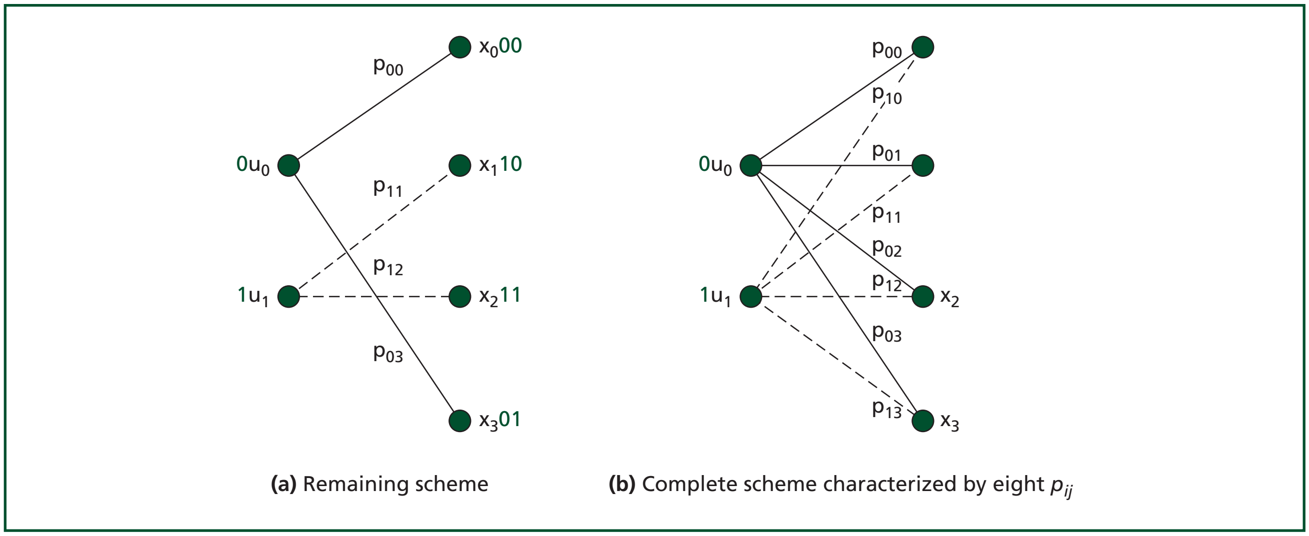

Figure 6.
Joint probability distribution of U and X.

is applied for the general case of coding superposition including all possible labeling schemes in a 4-PAM constellation. The shaping gain is evaluated, for target achievable rates, in terms of SNR savings that are related to SNR in a pair of good and bad users.

Maximum Private Message Achievable Rates by a 4-PAM Constellation for Superposition Coding

Figure 6 illustrates the joint probability distribution of U and X. The primary focus of this work is to extend our analysis to a case that is more general than that of modulation superposition using equiprobable symbols: we want to optimize the joint probability distribution $P_{UX}(u, x)$. The general case of superposition coding allows any mapping between U and X. $P_{UX}(u, x)$ is shown in Figure 6b where $p_{ij} = \Pr\{U = u_i, X = x_j\}$.

This is a highly non-linear problem with many optimization variables so we consider only a particular subset of solutions. For full generality, we consider all labeling schemes with a 4-PAM constellation when each user receives 2 symbols by associating two values of X for each value of U. P_{UX} is thus described completely by the three schemes for joint probability distribution described in Figure 5a, Figure 5b, and Figure 6a. The first two are similar to those obtained for modulation superposition, however the probabilities are unknown. The third possible scheme corresponds to the remaining possible labeling of the 4-PAM constellation, where each user can receive a maximum of two symbols. Clearly, this case does not correspond to the addition of two signals X_1 and X_2 carrying information to the corresponding user.

The region of private message achievable rates is composed of all convex combinations $\theta \cdot R_1 + (1 - \theta) R_2$ [4], where $\theta \in [0, 1]$. Since the right hand side inequalities of equation 3 and equation 4 are achievable, the evaluation of $\theta \cdot I(X; Y_1|U) + (1 - \theta) \cdot I(U; Y_2)$ for $\theta \in [0, 1]$ is sufficient to determine the region of achievable rates.

Now, we determine if higher rates are achievable using a constellation shaping technique. Therefore, the maximization has to be performed over the location of the transmit symbols $x_j \subset \mathcal{X}$ and over the joint probability distribution P_{UX} considering the three possible assignments previously discussed.

The maximum achievable rates are obtained by maximizing the multidimensional function,

$$\max_{P_{UX}, x_0, x_1, x_2 x_3} \theta \cdot I(X; Y_1 | U) + (1 - \theta) \cdot I(| U; Y_2) \qquad (10)$$

subject to the constraints defined in equation 7, where $\theta \in [0, 1]$. The mutual information of user 1 and of user 2 is given by equation 5 and is derived as a function of the unknown symbols $\{x_0, x_1, x_2, x_3\}$ and one probability p_{00}. The remaining probabilities can be deduced from equation 7. As an example, for the scheme illustrated in Figure 5a, the formulas from equation 7 are expressed as follows,

$$p_{00} + p_{01} + p_{12} + p_{13} = 1$$
$$p_{00} \cdot x_0 + p_{01} \cdot x_1 + p_{12} \cdot x_2 + p_{13} \cdot x_3 = 0$$
$$p_{00} \cdot x_0^2 + p_{01} \cdot x_1^2 + p_{12} \cdot x_2^2 + p_{13} \cdot x_3^2 = P \qquad (11)$$

This is a nonconvex optimization problem, which we solved using simulated annealing which provides a good approximation to the global optimum of a given function in a large search space. By applying this algorithm, a good approximation of optimal P_{UX} and the value of $\{x_0, x_1, x_2, x_3\}$ are found for the three labeling schemes considered above.

Simulation Results and Discussion

This section numerically compares the achievable rates, R_1 for user 1 (high SNR_1) and R_2 for user 2 (low SNR_2) in a case of modulation superposition with equiprobable symbols (denoted by MSEQ) and for optimal broadcast transmission with optimized probabilities and symbols considering all possible labeling schemes. The constellation shaping improvement will be evaluated in terms of attainable rate and of SNR improvement. For our analysis we consider the following cases in which the transmitted symbol probabilities have been optimized:

- *SCOP-I*. P_{UX} corresponds to Figure 5a.
- *SCOP-II*. P_{UX} corresponds to Figure 5b.
- *SCOP-III*. P_{UX} corresponds to Figure 6a.

The final result is the convex closure of the regions obtained in these three instances of superposition coding, which we refer to as an optimized case of SC, denoted by SCOP. The first two cases are compared with the similar scheme of equiprobable joint probabilities distribution. The comparisons are done under the same reception conditions and for various *SNR* pairs (SNR_1, SNR_2). The couples are obtained by fixing the *SNR* gap between the SNR of user 1 and the SNR of user 2 and for different values of SNR_2. The simulations are thus carried out by considering,

- *SNR* gap = {2, 3, 5, 7, 10}dB,
  SNR_2 = {2, 3, 4, 5, 6}dB and $\theta = [0{:}0.1{:}1]$.

The highest values of *SNR* gap correspond to a situation where the locations of user 1 and user 2 are far apart, whereas the lowest values represent a case in which the two users are closely spaced.

Figure 7 shows the maximum achievable rates for user 1 and user 2 for various scenarios. Note that Figure 7a shows improvement in the achievable rate closure region for (SNR_1, SNR_2) = (6 dB, 4 dB) when the constellation symbols and the symbol probabilities are jointly optimized with SCOP-I, compared to the case with MSEQ and $\alpha \leq 0.5$. In Figure 7b, the achievable rate region is not enhanced with joint optimization when comparing SCOP-II with MSEQ and $\alpha \geq 0.5$. In Figure 7c, the achievable rate region for SCOP-III, compared with the convex closure of the regions achievable in SCOP-I and SCOP-II, shows an improvement for certain values of θ. Thus, each case maximizes the achievable rate closure region over disjoint intervals of θ. For (SNR_1, SNR_2) = (6 *dB*, 4 *dB*) the region can be split into three parts and the achievable rates at the borders of zones are continuous,

- For $R_1 \in (0, 0.8)$, SCOP-I should be used ($0 < \theta \leq 0.5$),
- For $R_1 \in (0.8, 0.95)$, SCOP-III should be used ($0 < \theta < 0.7$),
- For $R_1 \in (0.95, 0.99)$, SCOP-II should be used ($0.7 \leq \theta \leq 1$).

The intuition behind the first two conclusions is rather clear. On one hand, for low rates of R_1, we should facilitate detection of user 2 using the SCOP-I scenario (positive symbols correspond to $U = u_0$ and negative ones to $U = u_1$), so there is an obvious separation of the data as a function of the symbols of U. On the other hand, to guarantee a high rate R_1, the symbols x_j associated with the detected variable U should be well separated, which is obtained by applying the SCOP-II scheme.

Figure 8 contrasts optimal joint probabilities with maximum achievable rates. As shown in Figure 8a, the corresponding probability distribution is approximately uniform when $\theta \geq 0.7$. For these values of θ, the rates achieved in the SCOP-II scheme are identical to those obtained with MSEQ ($\alpha \geq 0.5$). Moreover, we observed that the SCOP-II scheme achieves maximal rates compared to the rates obtained with SCOP-I or

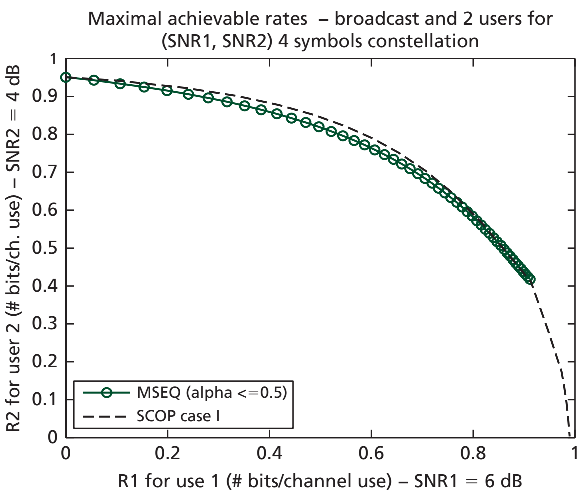

(a) MSEQ $\alpha \in$ *[0, 0.5]* with respect to SCOP case I

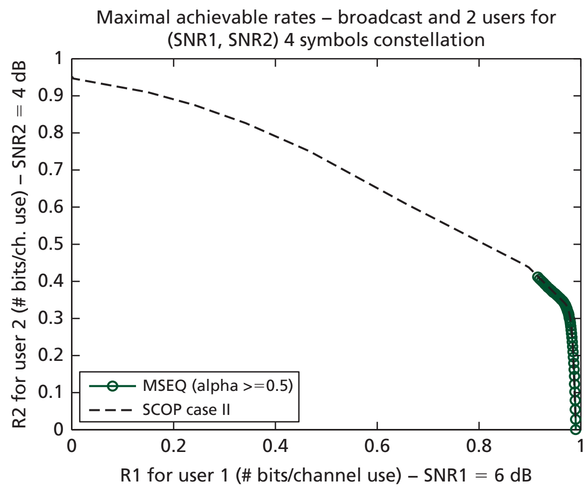

(b) MSEQ $\alpha \in$ *[0.5, 1]* with respect to SCOP case II

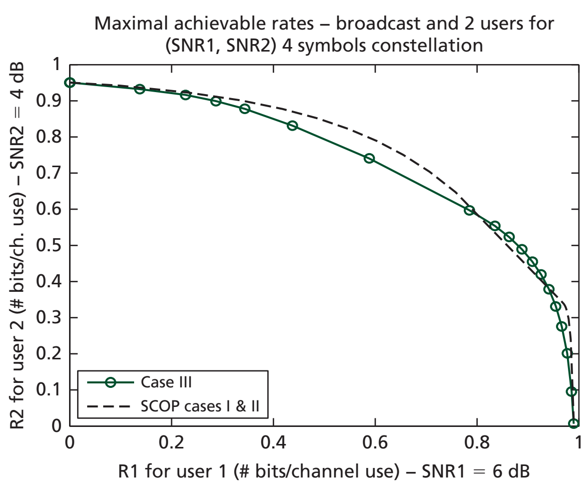

(c) SCOP case I and case II with respect to SCOP case III

MSEQ—Modulation superposition with equiprobable symbols
SC—Superposition coding
SCOP—SC optimized
SNR—Signal-to-noise ratio
SNRI—Signal-to-interference-plus-noise ratio

Figure 7.
Maximum achievable rates for users 1 and 2, SNR_1 = 6 dB and SNR_2 = 4 dB.

SCOP-III. Consequently, a uniform and symmetric distribution is optimal in the zone in which the data transmission of user 1 is favored. In the two other zones, where data transmission from user 2 is favored, the optimal probabilities of symbols near origin are higher than the ones for symbols far from origin. In contrast, the optimal symbols are non-uniform in all the three zones but remain symmetric ($x_0 = -x_3$ and $x_1 = -x_2$) for each theta considered. As an example at $\theta = 0.5$,

- Optimal $p_{00} = p_{13}$ is equal to 0.18 and optimal $p_{01} = p_{12}$ is equal to 0.32,
- Optimal $x_0 = -x_3$ is equal to 3.4 and optimal $x_1 = -x_2$ is equal to 1.1, and
- Optimal R_1 is equal to 0.706 and optimal R_2 is equal to 0.703.

Simulations done in the remaining configurations of (SNR_1, SNR_2) show results similar to the ones obtained in the case in which (SNR_1, SNR_2) = (6 dB, 4 dB).

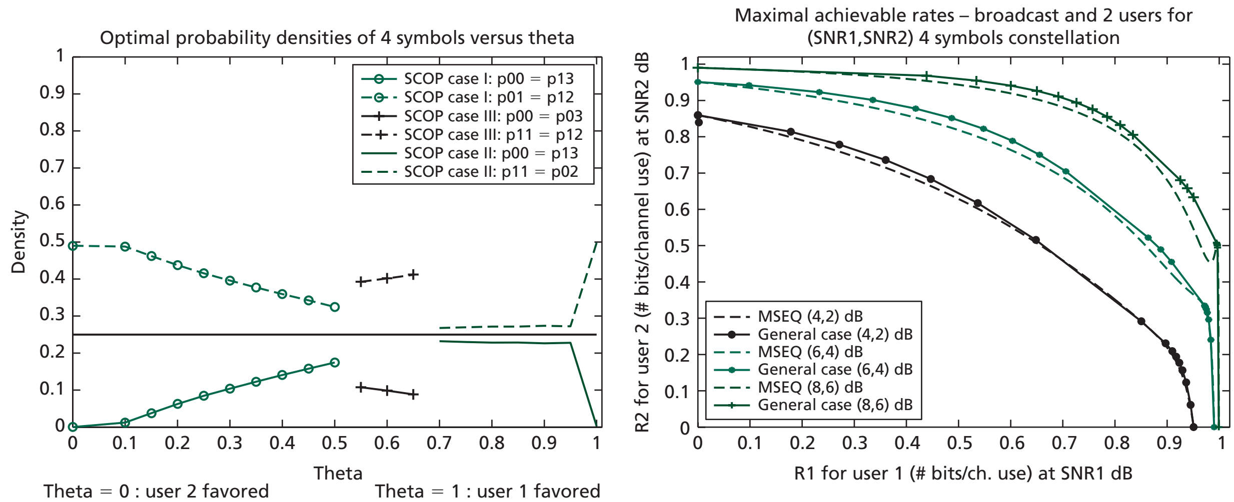

(a) Optimal joint probabilities (SCOP cases I, II, and III)

(b) Maximal achievable rates – general case w.r.t MSEQ

MSEQ—Modulation superposition with equiprobable symbols
SC—Superposition coding
SCOP—SC optimized
SNR—Signal-to-noise ratio
SNRI—Signal-to-interference-plus ratio

Figure 8.
Optimal joint probabilities and maximum achievable rates.

Each SCOP labeling scheme optimizes the achievable rate region for some value of θ in a 4-PAM setting. However the borders of the three regions vary when (SNR_1, SNR_2) changes. The numerical results also illustrate that the optimal symbol positions and joint probabilities are still symmetric about the origin. The optimal probabilities meet the constellation shaping principle.

A possible shaping gain in terms of achievable rates with a 4-PAM constellation is illustrated in Figure 8b for different couples of (SNR_1, SNR_2). The achievable rate region obtained in the cases with SCOP is consistently larger than the region obtained with MSEQ. To evaluate the contribution of constellation shaping, we compare the general case with MSEQ in terms of SNR savings for target achievable rates. The evaluation is done by using the following procedure composed of three steps:

1. We fix α and SNR_i with $i \subset \{1, 2\}$. The rate achieved by user i, denoted as $R_i^{MSeq.}$, when using MSEQ, is kept constant.
2. Then we determine the value of θ such that R_i^{Scopt} achieved by user i, when using SCOP, is equal to $R_i^{MSeq.}$ at SNR_i. Thus,

$$R_i^{Scopt.}(SNR_j, SNR_i, \theta) = R_i^{MSeq.}(SNR_j, SNR_i, \alpha) \quad (12)$$

3. Then we add a positive δ to SNR_j with $j \neq i$ until $R_j^{MSeq.}$ of user j coincides with R_j^{Scopt} achieved by user j at SNR_j in the optimized SC case. Thus,

$$R_j^{Scopt.}(SNR_j, SNR_i, \theta) = R_j^{MSeq.}(SNR_j + \delta_{opt}, SNR_i, \alpha) \quad (13)$$

The SNR increase yields δ_{opt} that is the SNR gain we seek.

Figure 9 provides a summary of SNR gains. Figure 9a summarizes the gains on SNR_1 assuming there is no rate loss and no SNR loss for user 2 obtained with SCOP compared with MSEQ. The comparisons are done for (SNR_1, SNR_2) equal to (4 dB, 2 dB), (6 dB, 4 dB) and (8 dB, 6 dB). Figure 9b illustrates the SNR_2 gain values assuming no rate and no SNR loss for user 1 in the same simulation scenarios.

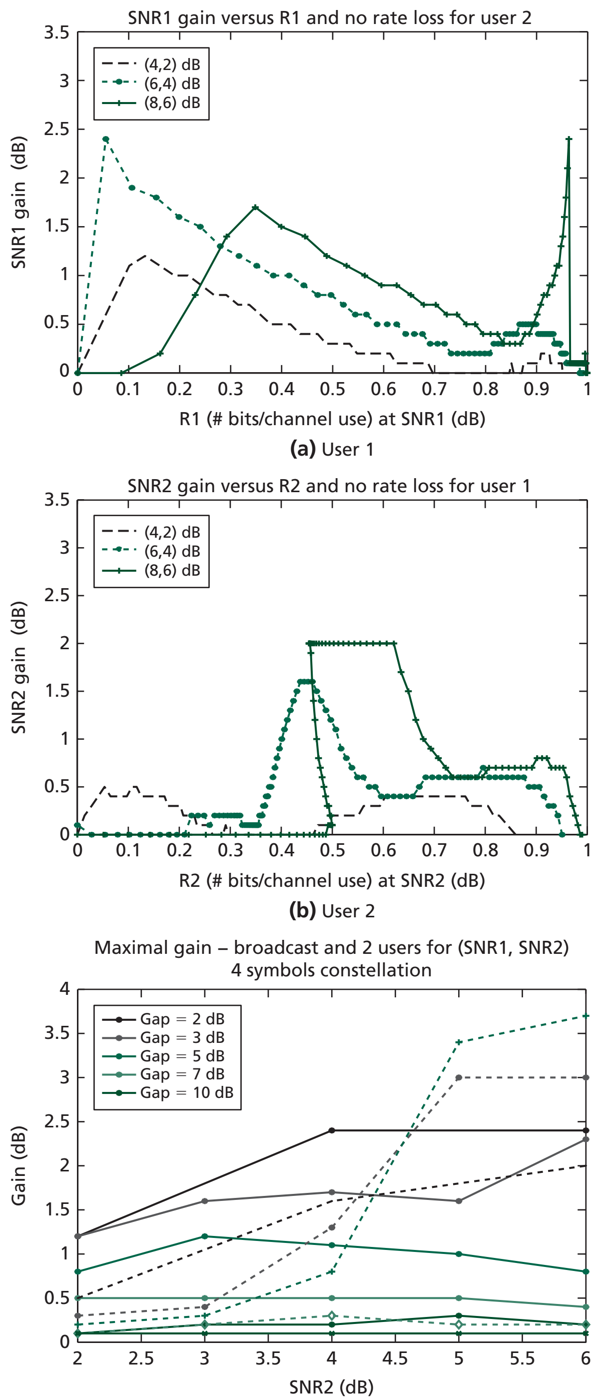

Figure 9.
SNR gains.

In both figures, maximal gains of 2.4 dB and of 2 dB are measured respectively for user 1 and for user 2. This maximal gain corresponds to a peak SNR in the case of user 1, and to several consecutive peaks in the case of user 2. For R_2 values around 0.5, the *SNR* gain oscillates between 0 dB and 2 dB. This oscillation can be explained by the fact that the sum rate curve achievable with finite inputs is not strictly increasing with α since the achievable rate for given bad channel conditions, i.e., for user 2, exhibit local minima and maxima [11]. It is shown that the number of local minima and maxima increases with SNR_2. The *SNR* gain is thus maximal for the couples of (R_1, R_2) for which α induces local minima for given couples of (SNR_1, SNR_2).

Figure 9c exhibits the maximal SNR gains obtained for all described scenarios. The highest achievable "maximal" gain is equal to 3.7 dB and is obtained for user 2 and for (11 *dB*, 6 *dB*). The curves show the maximal savings with joint optimization is at least equal to 1.5 dB on SNR for both users and for a small SNR gap (2 dB). **Figure 10** shows the average gain for user 1 and user 2 versus SNR. The curves for average SNR gain depicted in Figure 10a and in Figure 10b show that the highest SNR gains are obtained for the highest values of SNR_2 and when the SNR gap is lower than 5 dB for both users. An average gain up to 1 dB and 0.5 dB can be expected respectively for user 2 and user 1. The lower bound of average SNR gains is around 0.2 dB.

Use of the optimized SC scenario produces noticeable savings in SNR for the scenarios studied, although a small shaping gain in terms of achievable rate was observed for the 4-PAM constellation. The joint optimization of symbol probability density and constellation symbol positions contributes significantly to savings in SNR for both bad and good users exhibiting closed channel conditions, when superposition coding is used for a 4-PAM constellation.

Conclusion

In this paper, we derived the achievable rates for two broadcast transmission methods: 1) modulation superposition with uniformly distributed symbols with optimized joint probability density of the

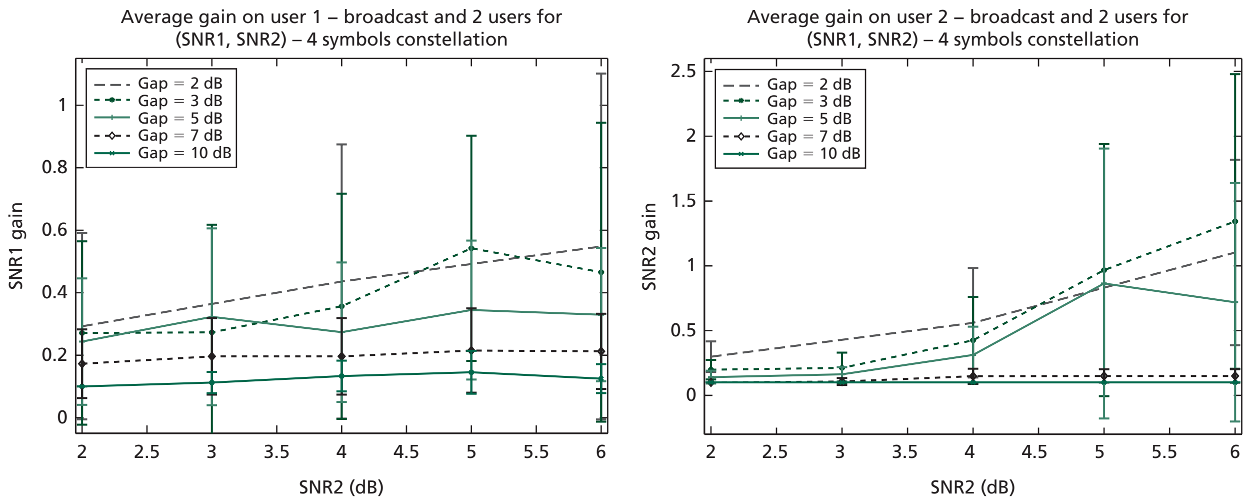

(a) Average gain on user 1 and no rate loss for user 2

(b) Average gain on user 2 and no rate loss for user 1

SNR—Signal-to-noise ratio

Figure 10.
Average gain on user 1 or user 2 versus SNR.

transmitted symbols, and 2) modulation superposition with uniformly distributed symbols with optimized constellation shape. We demonstrated that optimal broadcast transmission including this joint optimization yields slightly higher achievable rates in a 4-PAM setting. However, this small rate gain is translated into noticeable SNR savings of up to 3.5 dB at maximum and up to 1.2 dB in mean. The next step of this work will be to formulate a maximization problem for a standard modulation scheme in a 3G/LTE radio interface, more precisely, 16-QAM. This optimization will be achieved by taking into account a more general case of superposition coding. Preliminary results for modulation superposition including the first two labeling schemes considered have exhibited positive shaping gains on achievable rates and on SNR savings. We expect that for 16-QAM, by considering more labeling schemes, constellation shaping may lead to higher shaping gains. The work will be extended to a two-user fading Gaussian broadcast channel to provide results in a theoretical framework closer to the practical situation of unicast services transmission since a real world channel is never purely Gaussian.

References

[1] A. Agustin, J. Vidal, and O. Muñoz, "Performance of Downlink Schedulers with Superposed or Orthogonal Transmissions," Proc. IEEE Internat. Conf. on Commun. (ICC '10) (Cape Town, So. Afr., 2010).

[2] P. P. Bergmans and T. M. Cover, "Cooperative Broadcasting," IEEE Trans. Inform. Theory, 20:3 (1974), 317–324.

[3] A. R. Calderbank and L. H. Ozarow, "Nonequiprobable Signaling on the Gaussian Channel," IEEE Trans. Inform. Theory, 36:4 (1990), 726–740.

[4] E. Calvo, D. P. Palomar, J. R. Fonollosa, and J. Vidal, "The Computation of the Capacity Region of the Discrete Degraded BC Is a Nonconvex DC Problem," Proc. IEEE Internat. Symp. on Inform. Theory (ISIT '08) (Toronto, Ont., Can., 2008), pp. 1721–1725.

[5] Cisco, "Cisco Visual Networking Index: Global Mobile Data Traffic Forecast Update, 2010-2015," White Paper, 2011.

[6] T. M. Cover, "Broadcast Channels," IEEE Trans. Inform. Theory, 18:1 (1972), 2–14.
[7] European Telecommunications Standards Institute, "Digital Video Broadcasting (DVB), Framing Structure, Channel Coding and Modulation for Digital Terrestrial Television," ETSI EN 300 744.
[8] European Telecommunications Standards Institute, "Digital Video Broadcasting (DVB), System Specifications for Satellite Services to Handheld Devices (SH) Below 3 GHz," ETSI TS 102 585.
[9] G. D. Forney, Jr. and L.-F. Wei, "Multidimensional Constellations—Part I: Introduction, Figures of Merit, and Generalized Cross Constellations," IEEE J. Select. Areas Commun., 7:6 (1989), 877–892.
[10] R. K. Ganti, Z. Gong, M. Haenggi, C. Lee, S. Srinivasa, D. Tisza, S. Vanka, and P. Vizi, "Implementation and Experimental Results of Superposition Coding on Software Radio," Proc. IEEE Internat. Conf. on Commun. (ICC '10) (Cape Town, So. Afr., 2010).
[11] C. Huppert and M. Bossert, "On Achievable Rates in the Two User AWGN Broadcast Channel with Finite Input Alphabets," Proc. IEEE Internat. Symp. on Inform. Theory (ISIT '07) (Nice, Fra., 2007), pp. 2581–2585.
[12] International Telecommunication Union, Telecommunication Standardization Sector, "A Modem Operating at Data Signalling Rates of Up to 28,800 bit/s for Use on the General Switched Telephone Network and on Leased Point-to-Point 2-Wire Telephone-Type Circuits," ITU-T Rec. V.34, Sept. 1994, <http://www.itu.int>.
[13] H. Jin, R. Laroia, and T. Richardson, "Superposition by Position," Proc. IEEE Inform. Theory Workshop (ITW '06) (Punta del Este, Urug., 2006), pp. 222–226.
[14] F. Khan, "Broadcast Overlay on Unicast via Superposition Coding and Interference Cancellation," Proc. 64th IEEE Veh. Technol. Conf. (VTC '06-Fall) (Montreal, Que., Can., 2006).
[15] D. Kim, F. Khan, C. Van Rensburg, Z. Pi, and S. Yoon, "Superposition of Broadcast and Unicast in Wireless Cellular Systems," IEEE Commun. Mag., 46:7 (2008), 110–117.
[16] F. R. Kschischang and S. Pasupathy, "Optimal Nonuniform Signaling for Gaussian Channels," IEEE Trans. Inform. Theory, 39:3 (1993), 913–929.
[17] Y. Liu and C. Heneghan, "Optimization of Hierarchical Modulation for Use of Scalable Media," EURASIP J. Advances Signal Processing, 2010 (2010), Article ID 942638.
[18] J. N. Livingston, "Shaping Gains Using Non-Equiprobable Signaling," Proc. IEEE Global Telecommun. Conf. (GLOBECOM '90) (San Diego, CA, 1990), vol. 3, pp. 1994–1998.
[19] N. H. Ngo, S. A. Barbulescu, and S. S. Pietrobon, "Performance of Nonuniform M-ary QAM Constellation on Nonlinear Channels," Proc. 6th Australian Commun. Theory Workshop (AusCTW '05) (Brisbane, Aus., 2005), pp. 79–83.
[20] G. J. Pottie, "High Speed Digital Subscriber Lines: Preliminary Discussion of Shaping and Precoding for Single-Pair High Speed Digital Subscriber Lines," University of California contribution, ANSI T1E1.4/96-066, Apr. 22, 1996.
[21] V. Singh, On Superposition Coding for Wireless Broadcast Channels, Master of Science Thesis, Royal Institute of Technology (KTH), 2005.
[22] D. Sommer and G. P. Fettweis, "Signal Shaping by Non-Uniform QAM for AWGN Channels and Applications Using Turbo Coding," Proc. Internat. ITG Conf. on Source and Channel Coding (SCC '00) (Munich, Ger., 2000).
[23] X. Wang, J. Fu, J. Wang, C. Pan, and Z. Yang, "Shaping Gain for AWGN Channel by Non-Uniform Constellation in LDPC-Coded System," Proc. 11th IEEE Internat. Conf. on Commun. Syst. (ICCS '08) (Guangzhou, Chn., 2008), pp. 1302–1306.

(Manuscript approved December 2011)

ZEINA MHEICH is a Ph.D. candidate at CNRS/L2S

(Laboratoire de Signaux et Systèmes, Gif sur Yvette, France). She received her diploma in computer and communications engineering from the Lebanese University Faculty of Engineering, and her M.S. degree in advanced wireless communication systems from Université Paris-Sud in France. Her current research, conducted under the supervision of Dr. Pierre Duhamel, focuses on improving the achievable rate region for a finite alphabet input over a broadcast channel with additive white Gaussian noise by jointly optimizing the probability distribution of the constellation symbols and the constellation shape.

MARIE-LINE ALBERI MOREL is a research engineer in the Alcatel-Lucent Bell Labs' Networking and Networks research domain, and is based at Bell Labs' Centre de Villarceaux in Nozay, France. She received an M.S. degree in electronics and signal processing, and a Ph.D. degree in the signal processing field from Université Paris-Sud in France. During her Ph.D., she worked in the single input multiple output (SIMO) equalization field at Ecole Nationale de Statistique et d'Economie Appliquée (ENSEA). During her career at Alcatel-Lucent, she has contributed to various radio projects on problematic wireless local area network (WLAN) deployment, dimensioning for small cell networks, and most recently, on a fourth generation (4G) discontinuous networks project including caching technology. She also conducted research on DVB-SH mobile broadcast networks for the TéléVision Mobile Sans Limite French national project. Her current research focuses on the design of optimized solutions for video services delivery over mobile wireless networks and over converging 3GPP and DVB mobile broadcasting systems. She also serves as an assistant professor at Marne-La-Vallée University, France.

PIERRE DUHAMEL is research director of CNRS/L2S (Laboratoire de Signaux et Systèmes, Gif sur Yvette, France), where he is developing studies in signal processing for communications (including equalization, iterative decoding, multicarrier systems, cooperation) and signal/image processing for multimedia applications, including source coding, joint source/channel coding, watermarking, and audio processing. He is currently investigating the application of recent information theory results to communication theory. Dr. Duhamel has chaired and/or has served on the technical planning committees for numerous IEEE conferences and workshops in the field of signal processing. He has also served as an associate editor for the IEEE Transactions on Signal Processing and for IEEE Signal Processing Letters, as well as guest editor for the IEEE Transactions on Signal Processing special issue on Wavelets. He has published more than 80 papers in international journals, more than 250 papers in international conferences, and holds 28 patents. He is a co-author of the book Joint Source and Channel Decoding: A Cross Layer Perspective with Applications in Video Broadcasting. He has been a EURASIP fellow since 2008, and is a recipient of the "Grand Prix France Telecom" from the French Academy of Sciences. ◆

Appendix

The mutual information expression of user 1 and user 2, $I(X; Y_1|U)$ and $I(U; Y_2)$, depends on the scheme of the joint distribution of probability between U and X, P_{UX}, and the transition probability function, $P(y_k|x_i)$ with $k = \{1, 2\}$.

The transition probability function is expressed in the case of an AWGN channel for user 1 and user 2 as,

$$P(y_1|x_i) = \frac{1}{\sqrt{2 \cdot \pi \cdot \sigma_1^2}} \cdot \exp\left(-\frac{(y_1 - x_i)^2}{2\sigma_1^2}\right) \tag{A.1}$$

$$P(y_2|x_i) = \frac{1}{\sqrt{2 \cdot \pi \cdot \sigma_2^2}} \cdot \exp\left(-\frac{(y_2 - x_i)^2}{2\sigma_2^2}\right) \tag{A.2}$$

Case $\alpha \leq 0.5$ corresponds to the P_{UX} scheme in Figure 5a:

For a 4-PAM constellation, the coordinates of the four symbols are related to the total transmission power P and the splitting factor α:

$$\begin{aligned} x_0 &= \sqrt{\alpha \cdot P} + \sqrt{(1-\alpha) \cdot P} \\ x_1 &= -\sqrt{\alpha \cdot P} + \sqrt{(1-\alpha) \cdot P} \\ x_2 &= \sqrt{\alpha \cdot P} - \sqrt{(1-\alpha) \cdot P} \\ x_3 &= -\sqrt{\alpha \cdot P} - \sqrt{(1-\alpha) \cdot P} \end{aligned} \tag{A.3}$$

The uniform joint probabilities are written as,

$$p_{00} = p_{01} = p_{12} = p_{13} = 0.25 \tag{A.4}$$

Using equation 5, and A.1, A.2, A.3, and A.4, the mutual information of user 1 and user 2 can be derived as,

$$\begin{aligned} I(X; Y_1|U) = \int_{y_1=-\infty}^{+\infty} \Bigg[& p_{00} \cdot p(y_1|x_0) \log \frac{(p_{00} + p_{01}) \cdot p(y_1|x_0)}{p_{00} \cdot p(y_1|x_0) + p_{01} \cdot p(y_1|x_1)} \\ & + p_{01} \cdot p(y_1|x_1) \log \frac{(p_{00} + p_{01}) \cdot p(y_1|x_1)}{p_{00} \cdot p(y_1|x_0) + p_{01} \cdot p(y_1|x_1)} \\ & + p_{12} \cdot p(y_1|x_2) \log \frac{(p_{12} + p_{13}) \cdot p(y_1|x_2)}{p_{12} \cdot p(y_1|x_2) + p_{13} \cdot p(y_1|x_3)} \\ & + p_{13} \cdot p(y_1|x_3) \log \frac{(p_{12} + p_{13}) \cdot p(y_1|x_3)}{p_{12} \cdot p(y_1|x_2) + p_{13} \cdot p(y_1|x_3)} \Bigg] dy_1 \end{aligned} \tag{A.5}$$

and

$$\begin{aligned} I(U; Y_2) = & \\ & \int_{y_2=-\infty}^{+\infty} [p_{00} \cdot p(y_2|x_0) + p_{01} \cdot p(y_2|x_1)] \log \frac{p_{00} \cdot p(y_2|x_0) + p_{01} \cdot p(y_2|x_1)}{(p_{00} + p_{01})(p_{00} \cdot p(y_2|x_0) + p_{01} \cdot p(y_2|x_1) + p_{12} \cdot p(y_2|x_2) + p_{13} \cdot p(y_2|x_3))} \\ & + [p_{12} \cdot p(y_2|x_2) + p_{13} \cdot p(y_2|x_3)] \log \frac{p_{12} \cdot p(y_2|x_2) + p_{13}.p(y_2|x_3)}{(p_{12} + p_{13})(p_{00} \cdot p(y_2|x_0) + p_{01} \cdot p(y_2|x_1) + p_{12} \cdot p(y_2|x_2) + p_{13} \cdot p(y_2|x_3))} dy_2 \end{aligned} \tag{A.6}$$

Case $\alpha \geq 0.5$ corresponds to P_{UX} scheme in Figure 5b:
For a 4-PAM constellation, the coordinates of the four symbols are related to the total transmission power P and the splitting factor α:

$$\begin{aligned} x_0 &= \sqrt{\alpha \cdot P} + \sqrt{(1-\alpha)\cdot P} \\ x_1 &= \sqrt{\alpha \cdot P} - \sqrt{(1-\alpha)\cdot P} \\ x_2 &= -\sqrt{\alpha \cdot P} + \sqrt{(1-\alpha)\cdot P} \\ x_3 &= -\sqrt{\alpha \cdot P} - \sqrt{(1-\alpha)\cdot P} \end{aligned} \tag{A.7}$$

The uniform joint probabilities are written as,

$$p_{00} = p_{02} = p_{11} = p_{13} = 0.25 \tag{A.8}$$

Using equation 5, A.1, A.2, A.7, and A.8, the mutual information of user 1 and user 2 can be derived as,

$$\begin{aligned} I(X;Y_1|U) = \int_{y_1=-\infty}^{+\infty} \Bigg[& p_{00}\cdot p(y_1|x_0)\log\frac{(p_{00}+p_{02})\cdot p(y_1|x_0)}{p_{00}\cdot p(y_1|x_0) + p_{02}\cdot p(y_1|x_2)} \\ & + p_{02}\cdot p(y_1|x_2)\log\frac{(p_{00}+p_{02})\cdot p(y_1|x_2)}{p_{00}\cdot p(y_1|x_0) + p_{02}\cdot p(y_1|x_2)} \\ & + p_{11}\cdot p(y_1|x_1)\log\frac{(p_{11}+p_{13})\cdot p(y_1|x_1)}{p_{11}\cdot p(y_1|x_1) + p_{13}\cdot p(y_1|x_3)} \\ & + p_{13}\cdot p(y_1|x_3)\log\frac{(p_{11}+p_{13})\cdot p(y_1|x_3)}{p_{11}\cdot p(y_1|x_1) + p_{13}\cdot p(y_1|x_3)} \Bigg] dy_1 \end{aligned} \tag{A.9}$$

and

$$\begin{aligned} I(U;\, Y_2) = & \\ & \int_{y_2=-\infty}^{+\infty} [p_{00}\cdot p(y_2|x_0) + p_{02}\cdot p(y_2|x_2)]\log\frac{p_{00}\cdot p(y_2|x_0) + p_{02}\cdot p(y_2|x_2)}{(p_{00}+p_{02})(p_{00}\cdot p(y_2|x_0) + p_{11}\cdot p(y_2|x_1) + p_{02}\cdot p(y_2|x_2) + p_{13}\cdot p(y_2|x_3))} \\ & + [p_{11}\cdot p(y_2|x_1) + p_{13}\cdot p(y_2|x_3)]\log\frac{p_{11}\cdot p(y_2|x_1) + p_{13}\cdot p(y_2|x_3)}{(p_{11}+p_{13})(p_{00}\cdot p(y_2|x_0) + p_{11}\cdot p(y_2|x_1) + p_{02}\cdot p(y_2|x_2) + p_{13}\cdot p(y_2|x_3))} dy_2 \end{aligned} \tag{A.10}$$

We observe that the mutual information for user 1 and user 2 depends on α. Thus the achievable rate closure region can be obtained by varying α between 0 and 1.